

A scaling theory for the quasi-deterministic limit

David A. Kessler* and Nadav M. Shnerb†

Department of Physics, Bar-Ilan University, Ramat-Gan 52900 Israel

Deterministic rate equations are widely used in the study of stochastic, interacting particles systems. This approach assumes that the inherent noise, associated with the discreteness of the elementary constituents, may be neglected when the number of particles N is large. Accordingly, it fails close to the extinction transition, when the amplitude of stochastic fluctuations is comparable with the size of the population. Here we present a general scaling theory of the transition regime for spatially extended systems. Two fundamental models for out-of-equilibrium phase transitions are considered: the Susceptible-Infected-Susceptible (SIS) that belongs to the directed percolation equivalence class, and the Susceptible-Infected-Recovered (SIR) model belonging to the dynamic percolation class. Implementing the Ginzburg criteria we show that the width of the fluctuation-dominated region scales like $N^{-\kappa}$, where N is the number of individuals per site and $\kappa = 2/(d_u - d)$, d_u is the upper critical dimension. Other exponents that control the approach to the deterministic limit are shown to depend on κ . The theory is extended to include the corrections to the front velocity above the transition. It is supported by the results of extensive numerical simulations for systems of various dimensionalities.

PACS numbers: 87.23.Cc , 64.70.qj, 05.45.Xt, 05.45.-a

INTRODUCTION

The connection between a stochastic model of particle reactions (or equivalently, birth-death processes) and its associated deterministic rate equations is a topic of continuing interest. The common intuition is that the rate equations are not only qualitatively correct, but indeed provide, when the number of interacting particles is large, a quantitatively accurate approximation. This intuition is given concrete support by the Ω expansion of van Kampen [1]. However, there are a number of situations in which this picture is too naive and needs to be refined. One by now classic example of this is the exponentially small rate of extinction for a system with an absorbing state [2], which dominates the long-time dynamics, and is completely missed by the rate equations. Another example is the anomalously large corrections [3, 4] to the front velocity in stochastic systems which exhibit propagation into an unstable state; e.g., systems whose rate equation is the Fisher-Kolmogorov equation.

A system which captures features of both these examples is the spatially extended version [5] of the classic SIS (Susceptible-Infected-Susceptible) infection model of Weiss and Dishon [6]. In this model, contact (either on-site or nearest-neighbor) between an infected individual and a susceptible can, with some probability, convert the susceptible into an infected. Infected individuals spontaneously leave the infected state, reverting to susceptible. The well-mixed SIS system for sufficiently high infection probability possesses an endemic state, with an essentially constant level of infecteds, which however is subject to an exponentially small rate of extinction due to the existence of the absorbing state of zero infecteds. In addition, the deterministic rate equation is of Fisher-Kolmogorov type, and so a localized infection in the non-well-mixed case exhibits at the deterministic level an infection wave which propagates at constant velocity. However, the stochastic system exhibits not a bifurcation but rather a phase transition, characterized by the anomalous (for dimension $D < 4$) scaling exponents of the directed-percolation (DP) problem [7].

The connection between this complicated statistical behavior and the deterministic rate equations, which should be valid in the large- N limit (N being the total number of individuals, both susceptible and infected, on each site), is thus a natural topic for investigation, a study we initiated in a recent paper [5] (I). There we found that in one spatial dimension, the large- N behavior was governed by a scaling law with an exponent which we called $\kappa \approx 0.66$. For example, the phase transition point was shifted from the deterministic bifurcation point by an amount proportional to $N^{-\kappa}$. Investigating the correlation length, ξ , we found that there was a scaling collapse so that ξN^τ , with $\tau = 0.41$ was a function of N^κ times the distance to the deterministic bifurcation point.

In this paper, we show that this behavior is in fact a nonequilibrium version of what one may call the Ginzburg crossover. A fundamental concept in equilibrium field theory is that of the Ginzburg criterion, which states under which circumstances the noise is relevant. This is of course what predicts the existence of an upper critical dimension (UCD), above which the noise does not affect the long distance behavior and so the scaling is mean-field like. The logic underlying the Ginzburg criterion implies that if one could “dial” down the noise, the system would look more and more classical, and a crossover (which we will call the Ginzburg crossover) between the classical and noise-dominated regimes should become apparent, with the noise dominating the very long distance behavior (below the UCD, of

course). This program has been implemented in the context of the equilibrium finite-range Ising model, where spins interact with all their neighbors out to a distance R . As R increases, each spin is interacting with what is more and more closely approximating the mean-field, and mean-field behavior at short scales sets in. The problem can be carried out analytically for the finite-range spherical model [8], and has been investigated via simulation in the finite-range Ising model [9].

Another fundamental epidemics model considered in I is the SIR infection model of Kermack and McKendrick [10], where recovered individuals are immune to further infection. The critical behavior of this model is governed by the dynamic percolation exponents, with an upper critical dimension of 6. In I we have carried a numerical investigation of the SIR model also, showing that the theory converges, in the large N limit, to its mean-field limit with scaling exponents κ and τ that differ from those of the SIS (DP) model. Here we consider again the SIR model and derive analytically the relevant exponents using the same theory of the Ginzburg crossover, applied to the different universality class of the SIR model.

The main quantity used in the theory of epidemics to characterize the transmission potential of a disease is the basic reproduction rate R_0 , which is the expected number of secondary cases produced by a primary case in a population that is completely susceptible [11]. In the absence of demographic noise (e.g., in an infinite-dimensional model) the transition takes place at $R_0 = 1$. Noise shifts the transition to higher values of R_0 , but, as we will show below, the value $R_0 = 1$ still admits a special feature: the renormalized distance between $R_0 = 1$ and the actual transition point is N -independent as long as $\kappa < 1$. This interesting feature allows one to examine the scaling properties numerically in a very efficient manner, as it saves the effort needed to identify the location of the transition point for each N separately. This feature is utilized here when we compare the expected results with numerical simulations.

THE WELL MIXED SIS DYNAMICS AND THE TRANSITION ZONE

We first review the well-mixed version of the SIS model, and the relation of the stochastic model to the deterministic equations that determine the evolution of the system. Although this stochastic model has already been analytically solved, the discussion allows us to present the concepts that we intend to use below and to set the mathematical framework used in the study of the spatial models.

Let us consider a population of exactly N individuals, some of them are infected (I) and the rest are susceptible ($S = N - I$). The allowed processes are infection (with rate α/N , this is the type II model of [11]) and recovery (with rate β):



The corresponding master equation for the microscopic process can be formulated in terms of P_n , the chance to have n infected individuals:

$$\dot{P}_n = \beta(-nP_n + (n+1)P_{n+1}) + \frac{\alpha}{N}[-n(N-n)P_n + (n-1)(N-(n-1))P_{n-1}]. \quad (2)$$

Defining $\langle I \rangle = \sum_n nP_n$ as the expected number of infecteds, one finds after index rearrangement:

$$\langle \dot{I} \rangle = -\beta\langle I \rangle + \frac{\alpha}{N} \sum_n n(N-n)P_n = (\alpha - \beta)\langle I \rangle - \frac{\alpha}{N}\langle I^2 \rangle. \quad (3)$$

The essence of the van Kampen Ω expansion is that this equation closes if $\langle I \rangle \gg 1$, so that the variance of I makes a negligible contribution, giving the standard logistic equation

$$\langle \dot{I} \rangle = (\alpha - \beta)\langle I \rangle - \frac{\alpha}{N}\langle I \rangle^2. \quad (4)$$

Since $0 \leq \langle I \rangle \leq N$, it is necessary for N to be large, in order for the rate equation, Eq. (4), to be valid. This, however, is not sufficient. If $\alpha > \beta$, Eq. (4) has an attractive fixed point at $\langle I \rangle = I_0 = N(1 - 1/R_0)$, where $R_0 \equiv \alpha/\beta$ is the primary reproductive number and I_0 is indeed large if N is large, as required. Although the system admits an absorbing state at $I = 0$, the chance of a giant fluctuation that takes the system from I_0 to zero is exponentially small in I_0 , thus when $N \rightarrow \infty$ stochastic extinction (fadeout) is impossible once the system reaches its steady state. However, if the number of infected individuals in the initial state is small, stochastic effects are transiently present even in the $N \rightarrow \infty$ limit. For example, introducing one infected individual results in either short-time extinction

(with probability $1/R_0$) or an endemic state (with probability $(R_0 - 1)/R_0$). If $R_0 = 1$ exactly, at the $N \rightarrow \infty$ limit the system performs an unbiased random walk in n , the number of infecteds, and the theory of first passage times tells us that the chance of extinction is still unity, but the probability $P(q)$ to have q infection events scales like $q^{-3/2}$.

At finite N the situation is more complex. Now the steady state of Eq. (4) corresponds to a finite number of infected individuals in the endemic state, which mean that a finite, but large, fluctuation may cause a fadeout. The chance for such a fadeout is large when R_0 is close to one, i.e., when the attractive fixed point corresponds to only a few individuals. Instead of having a sharp extinction to proliferation transition at $R_0 = 1$, now the transition is “soft”: defining $\tilde{\Delta} = R_0 - 1$ as the distance from the transition, $I_0 \sim N\tilde{\Delta}$; a metastable state exists only if this quantity (the distance of the stable solution from the absorbing state) is larger than the typical fluctuation size, \sqrt{N} , thus a transition *zone* of width $\tilde{\Delta} \sim N^{-1/2}$ occurs between the extinction and the proliferation regimes. As shown in [12], $P(q)$ decays exponentially in the extinction phase $\tilde{\Delta} < 0$, has a peak at $\exp(\text{const} \cdot N)$ at the endemic phase $\tilde{\Delta} \gg 1/\sqrt{N}$, and decays like $q^{-3/2}$ with a cutoff at N in the transition zone. Note that the width of the transition zone goes to zero as N approaches infinity, recovering the sharp transition at $\tilde{\Delta} = 0$ that characterizes the deterministic theory.

THE ABSENCE OF SELF-INTERACTION

The derivation of Eq. (4) from Eq. (3) involves the neglect of $\mathcal{O}(1/N)$ terms. In particular one can easily see that the rate of infection when only one infected individual appears in a population of size N is $\alpha(1 - 1/N)$, so the transition occurs at $R_0 = 1 + 1/N$. This result reflects the most trivial effect of discretization, namely, the absence of self-interactions [13]: an infected individual cannot infect itself, so the effective size of the population “seen” by the first infected is $N - 1$ instead of N . There are presumably other nonsingular $1/N$ corrections to the transition point, but for convenience we will refer to all these $1/N$ corrections as the “self-interaction” effect.

Putting this fact together with the discussion of the last section, we realize that there are two N dependent functions that control the transition: one is the $\mathcal{O}(1/N)$ shift of the transition point, the other is the width of the “quantum” regime (the region above the transition point in which the system is controlled by demographic fluctuations) that scales, in the well-mixed limit, like $N^{-1/2}$. As $N \rightarrow \infty$ the shift is negligible with respect to the width of the transition zone, so there is only one scale in the problem, $\Delta \sim N^{-1/2}$. However this behavior is not generic. As we will show below, in some cases the width of the transition zone is much *narrower* than $1/N$, and in these cases one should take into account the two scales.

SPATIAL SIS MODEL AND THE TRANSITION ZONE

What happens if the system is extended? For the sake of concreteness let us focus on the example of an infinite one dimensional array of patches with N individuals on each patch. The probability per unit time of a susceptible on the n th site being infected by a given sick agent residing at this site is $\alpha(1 - \chi)/N$ and of being infected by a given infected resident of one of the neighboring sites is $\alpha\chi/2N$ (in a d dimensional system, this chance will be $\alpha\chi/Nd$). This corresponds to the “travelers model” considered in Ref. [14]. The deterministic rate, or mean-field (MF), equations, are

$$\begin{aligned} \dot{I}_n &= -\beta I_n + \frac{\alpha(1 - \chi)}{N} I_n (N - I_n) + \frac{\alpha\chi}{2N} (N - I_n) (I_{n+1} + I_{n-1}) \\ &= \frac{\alpha\chi}{2} \nabla^2 I + (\alpha - \beta) I_n - \frac{\alpha}{N} I_n^2 + \frac{\alpha\chi}{2N} I \nabla^2 I \end{aligned} \quad (5)$$

where ∇^2 stands for the discrete version of the Laplacian operator. The last, nonlinear diffusion, term, does not materially affect the dynamics (naive dimensional analysis shows that it is an irrelevant operator). Without this term one recognizes, on the MF level, the celebrated Fisher (or FKPP [15]) equation for invasion of a stable into an unstable phase, with a sharp transition at $\alpha = \beta$ (or $R_0 \equiv \alpha/\beta = 1$), and front propagation with a velocity of $2\sqrt{\alpha\chi\beta\tilde{\Delta}/2}$, since the effective diffusion constant is $\alpha\chi/2$ and the net growth rate is $\alpha - \beta = \beta\tilde{\Delta}$.

What happen when stochasticity is taken into account? If $N = 1$, i.e., there is only one agent on any site and so all infections are nearest-neighbor (thus it is reasonable to take $\chi = 1$), the stochastic process is known as the contact process, which undergoes a continuous phase transition from extinction to proliferation. The “effective” infection rate is smaller than α , since a sick agent cannot infect its neighbor if it is already sick. The transition happens at some

$R_c > 1$, e.g., here for $N = 1$, $R_c \approx 3.297$. While the exact value of R_c is of course non-universal, the extinction transition, which belongs to the directed percolation equivalence class [7], admits three universal critical exponents:

1. The spatial correlation length diverges as $|\Delta|^{-\nu_\perp}$, where we introduce $\Delta \equiv R_0 - R_c$ as the distance from the stochastic transition, as opposed to $\tilde{\Delta}$, which measures the distance to the *mean-field* transition; in 1d, $\nu_\perp \approx 1.09$
2. The temporal correlation length diverges like $|\Delta|^{-\nu_\parallel}$; in 1d, $\nu_\parallel \approx 1.73$
3. Above the transition the steady state density of infecteds, I_0 , grows like Δ^β ; in 1d, $\beta \approx 0.28$

The values of these critical exponents depend only on the dimensionality of the system and not on the microscopic details of the process. Above the critical dimension $d = 4$ the exponents take their MF values, $\nu_\perp = 1/2$, $\nu_\parallel = 1$, $\beta = 1$.

As N (the number of agents on a site) increases, demographic fluctuations become smaller. In the infinite N limit one recovers the MF transition described in Eq. (5). First, the transition point moves back to $R_c = 1$; second, the values of the critical exponent in this deterministic limit are equal to their MF values. For example it is clear from Eq. (5) that above the transition the density scales linearly with Δ , i.e., that $\beta = 1$. Below the transition I is small and the nonlinear term in Eq. (5) is negligible, hence if $I(x, 0) = \delta(x)$, $I(x, t) \sim \exp(-x^2/2Dt - \Delta t)$. The maximal density at x occurs when $t \sim x/\sqrt{\Delta D}$; thus the spatial profile of *total* infections is proportional to $\exp(-x/\xi_\perp)$ with $\xi_\perp \sim 1/\sqrt{\Delta}$, so that $\nu_\perp^{MF} = 1/2$.

At any finite N , though, close enough to R_c the system is controlled by stochastic effects, as implied by universality. As N becomes large, the effects of stochasticity are restricted to a narrow region close to the transition point, which defines the width of the transition (“quantum”) zone.

In I, we have shown numerically that close to the transition point the spatial correlation length is given by:

$$\xi_\perp = AN^{-\tau}(R_c - R_0)^{-\nu_\perp} \quad (6)$$

where the transition takes place at $R_c = 1 + BN^{-\kappa}$. The values $\kappa \approx 0.66$ and $\tau \approx 0.41$ have been obtained numerically for different microscopic models that belongs to the DP equivalence class and seem to be identical for the different models up to the accuracy of the numerics. As long as $\kappa < 1$, the region in the parameter space in which the system is controlled by stochasticity coincides with the interval between the stochastic and the deterministic critical points; i.e., it also scales like $N^{-\kappa}$. Rescaling appropriately the correlation length and the distance from the transition, our numerics (see I) showed an whole scaling regime described by the function:

$$N^{\kappa-\tau/\nu_\perp}\xi_\perp^{-1/\nu_\perp} = \mathcal{F}(\tilde{\Delta}N^\kappa) \quad (7)$$

The scaling function \mathcal{F} vanishes linearly at a positive value of its argument, which marks the transition point. Notice that what enters here is $\tilde{\Delta} \equiv R_0 - 1$, so that the behavior at the classical transition point is controlled by the fluctuations, even though it is outside the range of the linear behavior of \mathcal{F} . We will see later that the story is more complicated for $\kappa > 1$.

As discussed in the introduction, this scaling behavior is the result of a crossover between the deterministic theory and the critical theory as the critical point is neared. We will now use this to derive a scaling relation between τ and κ . Then we will obtain the value of κ by calculating the Ginzburg criterion for the model.

To connect τ to κ , one observes that the scaling function $\mathcal{F}(x)$ takes us from the stochastic regime at finite x (close to the transition) to the deterministic regime at large negative x , corresponding to the region deeply below the transition. Even for $|x|$ large, the system may still be arbitrary close to the transition ($\tilde{\Delta}$ may be arbitrarily small) as long as N is large enough. This implies that in the $x \rightarrow -\infty$ limit, the correlation length must diverge like $\tilde{\Delta}^{-1/2}$, *independent of N* . As a result the leading behavior of $\mathcal{F}(x)$ at large negative x must obey $\mathcal{F}(x) \sim x^{1/2\nu_\perp}$. To cancel the N dependence in the expression

$$N^{\kappa-\tau/\nu_\perp}\xi_\perp^{-1/\nu_\perp} = \Delta^{1/2\nu_\perp}N^{\kappa/2\nu_\perp} \quad (8)$$

one must have the scaling relation

$$\tau = \kappa \left(\nu_\perp - \frac{1}{2} \right). \quad (9)$$

Given that we found $\kappa \approx 0.66$, this implies a value of $\tau \approx .40$, consistent with our numerical findings. This scaling relation also implies that we can rewrite Eq. (7) as

$$\xi = N^{\kappa/2} \left[\mathcal{F}(\tilde{\Delta}N^\kappa) \right]^{-\nu_\perp} \quad (10)$$

A similar argument is applicable to any of the quantities that diverge at the transition. One example that will be used below is the overall "mass" M_N of a cluster, namely the average total number of infection events before extinction. Utilizing the same scaling analysis, and the known mean field dependence $M_N = 1/\tilde{\Delta}$, one expects that for $\kappa < 1$,

$$M_N \sim N^\kappa \left[\mathcal{G} \left(\tilde{\Delta} N^\kappa \right) \right]^{-\gamma} \quad (11)$$

where \mathcal{G} vanishes linearly at the transition point, and ϕ_M is the critical scaling exponent for the mass,

$$\gamma \approx 1.24 \quad (12)$$

Eq. (11) is a useful relation that allows us to recover κ directly from numerical simulations at fixed R_0 . To demonstrate the critical exponents one has to locate exactly the transition point for any value of N ; this is indeed a very tedious task. Instead, we can choose to simulate exactly at $R_0 = 1$, which in our case implies $R_0 = 1$. At this point the argument of the scaling function is exactly zero, independent of N , so the mass scales like N^κ . A plot of M_N/N^κ vs. N at $R_0 = 1$ must converge to a constant in the large N limit. Below we will test this condition to verify numerically the predictions of our theory for κ , as explained in the next section.

However, this strategy works only for $\kappa < 1$. As explained above, for higher values of κ the trivial self-interaction shift of the transition point is not negligible in the $N \rightarrow \infty$ limit. Thus, as will be exemplified below, for dimensions where $\kappa > 1$ one has to find first the transition point at $R_c = 1 + \mathcal{O}(1/N)$, and only near that point the transition region manifests itself.

THE EXPONENT κ AND THE GINZBURG CROSSOVER

Determining κ , thus, is enough to know everything about the quasi-deterministic regime. To find the value of κ we adopt here a Ginzburg criterion approach, looking for the leading perturbative correction in inverse powers of N , and associate the stochastic regime with the region where this leading correction is $\mathcal{O}(1)$.

As a platform for the perturbative analysis we have chosen the Peliti-Doi field theoretic technique [16] (see [17] for details). Starting with the master equation for the SIS process, at a single site (zero dimensional system) with N individuals presented above. Eq. (2) may be written as

$$\dot{\psi} = -\mathcal{H}\psi \quad (13)$$

where

$$\psi \equiv \sum_n P_n |n\rangle. \quad (14)$$

Using the creation-annihilation operators $a|n\rangle = n|n-1\rangle$ and $a^\dagger|n\rangle = |n+1\rangle$, the "Hamiltonian" takes the form

$$\mathcal{H}/\beta = (a^\dagger a - a) + R_0(a^\dagger a - a^\dagger a^\dagger a) + \frac{R_0}{N}(a^\dagger - 1)(a^\dagger a a^\dagger a). \quad (15)$$

Using the commutation relation $[a^\dagger, a] = 1$ and shifting from a^\dagger (that have a vacuum expectation value of unity [17]) to $\bar{a} = a^\dagger - 1$ one obtains:

$$\mathcal{H}/\beta = (1 - R_0(1 - \frac{1}{N}))\bar{a}a - R_0(1 - \frac{1}{N})\bar{a}\bar{a}a - \frac{R_0}{N}(\bar{a}\bar{a}\bar{a}aa + 2\bar{a}\bar{a}aa + \bar{a}aa). \quad (16)$$

The first, "mass" term of the Hamiltonian determines the transition point: the system is in the active phase when the (renormalized) mass becomes negative. If $N \rightarrow \infty$, an outbreak may occur at $\alpha > \beta$, i.e., the transition happens when $\tilde{\Delta} = R_0 - 1 = 0$. The $1/N$ correction to this result reflects, again, the absence of self-interactions.

Formally, the time evolution of ψ is given by:

$$\psi(t) = e^{-Ht}\psi(t=0). \quad (17)$$

With the aid of time slicing and the coherent state representation one may arrive at a path integral representation of the evolution in time where the former creation-annihilation operators are replaced by complex-valued fields defined over a continuous space-time [17]:

$$\psi(t) = \int \mathcal{D}a\mathcal{D}\bar{a} e^{-\mathcal{S}_0(\bar{a},a) - \mathcal{S}_1(\bar{a},a)} \psi(0) \quad (18)$$

where

$$\mathcal{S}_0 = \int d^d x dt \bar{a}(\vec{x}, t) [\partial_t - D\nabla^2 - m] a(\vec{x}, t). \quad (19)$$

with $m = \tilde{\Delta} - \frac{R_0}{N}$ and

$$\mathcal{S}_1 = R_0 \int d^d x dt \left[\left(1 - \frac{1}{N}\right) \bar{a} \bar{a} a - \frac{1}{N} (\bar{a} \bar{a} \bar{a} a a + 2 \bar{a} \bar{a} a a a + \bar{a} a a a a) \right]. \quad (20)$$

The renormalized values for all the constants in the problem may be obtained perturbatively by averaging over the cumulant expansion of $\exp(-\mathcal{S}_1)$ with weight $\exp(-\mathcal{S}_0)$. The free propagator, in terms of spatial Fourier components, is

$$\langle \bar{a}(k', t') a(-k, t) \rangle = \delta(k' + k) \theta(t - t') e^{(-k^2 + m)(t - t')}. \quad (21)$$

Here we are not really interested in the exact values of the perturbative corrections. All we are looking for is the width of the transition zone in the limit $\tilde{\Delta} \rightarrow 0$ and $N \rightarrow \infty$. If a perturbative correction is proportional to $N^{-y} \tilde{\Delta}^{-x}$, this correction becomes important (i.e., of order unity) when $\tilde{\Delta} = N^{-y/x}$. There are many possible perturbative corrections with different x and y , but κ is determined by the one that corresponds to the minimal value of y/x . In appendix 1 we will analyze the various elements of the perturbative expansion and conclude that

$$\kappa = \frac{2}{4 - d}; \quad (22)$$

in particular κ is $2/3$ in one dimension, with almost perfect agreement with the numerical results reported in I. Moreover our result for a well mixed system (zero dimensions) is indeed $\kappa = 1/2$, again with perfect agreement with the known results in that case.

For 2d SIS, our expression predicts $\kappa = 1$, so that the size of the stochastic regime is of the same order as the self interaction $1/N$ corrections. As shown above, κ determines also the relation between the average size of the epidemic and N when the infection rate takes its $N \rightarrow \infty$ critical value, $R_0 = 1$. Thus, in this case, we expect $M_N \sim N$. The data for this is presented in Fig. 1. The results are indeed consistent with the prediction; however the convergence is quite slow, much slower than in 0 and 1 dimensions.

In three dimensions, $\kappa > 1$ and so the transition region is smaller than the $\mathcal{O}(1/N)$ (self interaction) shift in the transition point. This leads to an interesting situation where there are two separate scaling regimes for large N . We will return to this point after first discussing the case of the SIR model.

THE SUSCEPTIBLE-INFECTED-RECOVERED (SIR) MODEL ON SPATIAL DOMAINS.

The other classic model of epidemics is the SIR model, which assumes that a recovered (R) individual cannot be infected again, so it is removed irreversibly from the "pool" of susceptible. The basic processes are:



The corresponding master equation for the microscopic process in a well-mixed population can be formulated in terms of m , the number of susceptibles, and n , the number of infected individuals:

$$\dot{P}_n = \beta (-n P_{m,n} + (n+1) P_{m,n+1}) + \frac{\alpha}{N} (-n m P_{m,n} + (n-1)(m+1) P_{m+1,n-1}). \quad (24)$$

In the deterministic limit, with the definition $S = \sum_m m P_{m,n}$ and $I = \sum_n n P_{n,m}$ and neglecting correlations ($\overline{nm} = \bar{n}\bar{m}$) one gets the equations:

$$\dot{S} = -\frac{\alpha}{N} S I \quad \dot{I} = -\beta I + \frac{\alpha}{N} S I \quad \dot{R} = \beta I, \quad (25)$$

where the last equation is just a consequence of the I dynamics. Since $S = N - R - I$, the two coupled equations, (again introducing $\tilde{\Delta} = \alpha/\beta - 1$):

$$\dot{I} = \beta \tilde{\Delta} I - \frac{\alpha}{N} I^2 - \frac{\alpha}{N} I R \quad \dot{R} = \beta I, \quad (26)$$

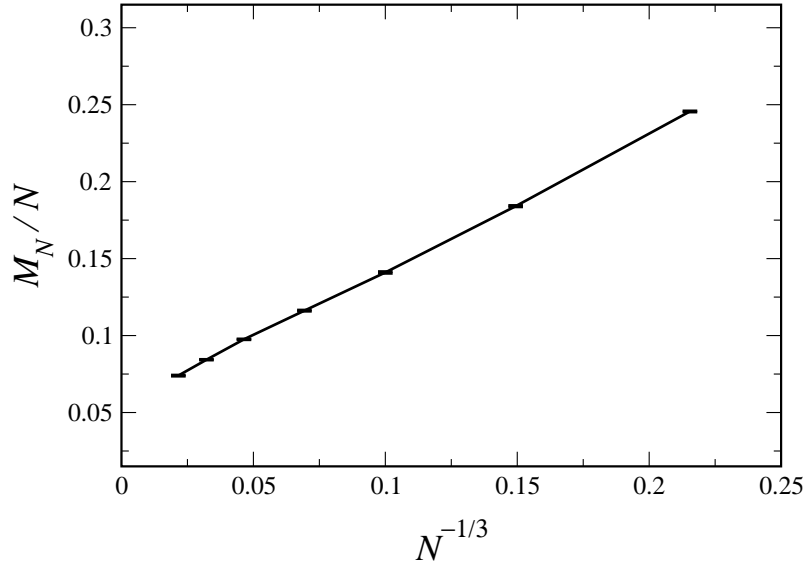


FIG. 1: The scaled “mass” of the aggregate, M_N/N , for the SIS model in two dimensions. The Ginzburg analysis suggests that, for large N , this ratio approaches a constant. Indeed, the plot shows that as N increased the ratio converges to a finite value. However this convergence is very slow, as implied by the $N^{-1/3}$ scaling of the abscissa.

are enough to describe the system. The SIR dynamics does not support a nontrivial equilibrium steady state; instead at any site the epidemic disappears when $t \rightarrow \infty$, leaving a finite density of recovered behind. This is manifested by the irreversible dynamics of R .

Clearly, given $I(x, t)$ one can solve for the number of recovered individuals at x :

$$R(x, t) = \beta \int_0^t I(x, \tau) d\tau, \quad (27)$$

Plugging that into Eq. (26) and adding terms that represent migration and discrete noise one gets:

$$\dot{I} = D\nabla^2 I + \beta\tilde{\Delta}I - \frac{\alpha}{N}I^2 - \frac{\alpha\beta}{N}I \int_0^t I(\tau) d\tau + \eta(x, t)\sqrt{I} \quad (28)$$

where η is a delta-correlated noise, and $D = \alpha\chi/2$ is the effective diffusion constant. Naive scaling analysis of Eq. (28) shows that the I^2 term is irrelevant and that the noise term becomes relevant when $d \leq 6$, as expected from the mapping to the dynamic percolation problem. Following [18] we integrate both sides of Eq. (28) from $t = 0$ to ∞ , using $\int \dot{I} dt = 0$ and $\int_0^\infty I(t) \int_0^t I(\tau) dt d\tau = 1/2[\int_0^\infty I(t) dt]^2$, we arrive at

$$D\nabla^2\Phi + \beta\tilde{\Delta}\Phi - \frac{\alpha\beta}{2N}\Phi^2 + \zeta(x)\sqrt{\Phi} = 0. \quad (29)$$

where $\Phi(x) \equiv \int_0^\infty I(x, t) dt$. Note that the variance of the noise term in Eq. (29) must satisfy

$$\overline{\text{Noise}^2} = \int_0^\infty dt_1 \int_0^\infty dt_2 \overline{\eta(t_1)\eta(t_2)} \sqrt{I(t_1)}\sqrt{I(t_2)} = \int_0^\infty dt_1 I(t_1) = \Phi \quad (30)$$

justifying the form of the noise amplitude term in the Φ equation. Rescaling Eq. (29) by N we have (now $m \equiv \beta\tilde{\Delta}$),

$$D\nabla^2\Phi + m\Phi = \frac{\alpha\beta}{2}\Phi^2 + \frac{1}{\sqrt{N}}\zeta(x)\sqrt{\Phi}. \quad (31)$$

Eq. (31) may be analyzed perturbatively, as shown by [18], by the same diagrammatic expansion used for the directed-percolation case (see Appendix 1) where the only difference is that the free propagator, instead of Eq. (21),

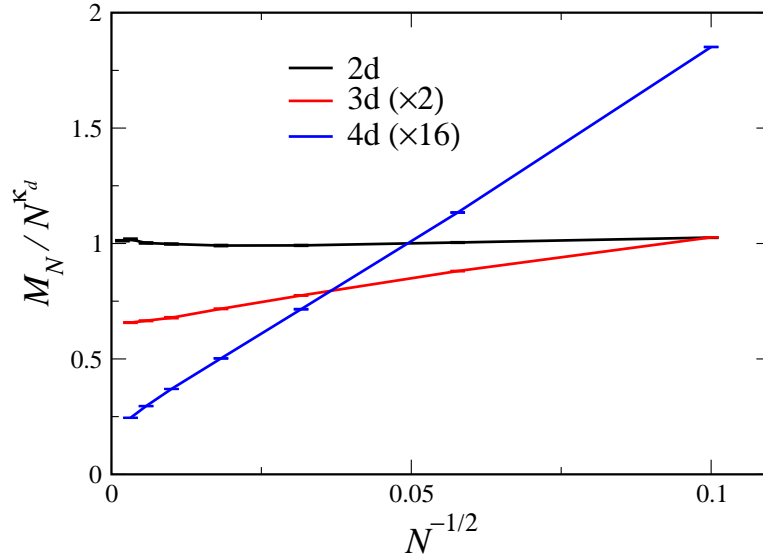


FIG. 2: The scaled “mass” of the aggregate, M_N/N , for the SIR model in $D = 2, 3$, and 4 , showing the convergence to a finite value in the limit $N \rightarrow \infty$.

is

$$\langle \Phi(k)\Phi(k') \rangle = \delta(k' + k) \frac{1}{k^2 + m}. \quad (32)$$

The first correction to the diffusion constant comes from the same self-energy diagram shown in Fig. 7, but here the correction is $[N\tilde{\Delta}^{\frac{6-d}{2}}]^{-1}$, thus $\kappa = 2/(6-d)$. Accordingly, in both the SIR and SIS cases, we have that

$$\kappa = \frac{2}{d_u - d}, \quad (33)$$

where d_u is the upper critical dimension.

This result is consistent with the exact scaling of the transition region in SIR in 0 dimensions, namely $\kappa = 1/3$ [19]. It is also consistent with our numerical findings in I for the case of one dimension, where we found $\kappa \approx 0.41$, to be compared with our prediction of $2/5$. We can test our prediction for higher dimensions by again measuring the total mass at the classical transition point divided by N^κ . This is presented in Fig. 2. The results are seen to converge relatively quickly to its finite $N = \infty$ value in two and three dimensions, but show, similar to the SIS case in two dimensions, a very slow convergence in four dimensions.

THE CASE OF $\kappa > 1$

As we have seen above, two scales are involved in the large N limit. One is the shift of the transition point due to the absence of self-interactions, and this leads to $1/N$ corrections for the critical reproductive number R_c , and the other is the width of the “quantum” regime where fluctuations dominate the system behavior, the width of this region scales like $N^{-\kappa}$. For $d < d_u - 2$ we obtained $\kappa < 1$ and the quantum regime is wider than the self-interaction shift, thus the effect of self-interactions is negligible. If $d = d_u - 2$ both corrections scale like N^{-1} and this leads to the slow convergence of the results to the large N limit. We still have to consider the case where $\kappa > 1$, i.e., where the quantum regime is narrower than the self interaction shift.

For the SIS and SIR dynamics considered here, and for an integer number of dimensions, we have to consider the case $\kappa = 2$ for $d = d_c - 1$ (3d for SIS, 5d for SIR) and $\kappa = \infty$ at the upper critical dimension.

At $d = d_u$ the situation is trivial: $\kappa = \infty$ means that the width of the transition zone is zero, since the system behaves (up to logarithmic corrections) like its mean-field (infinite dimensional) limit. Note the difference between a

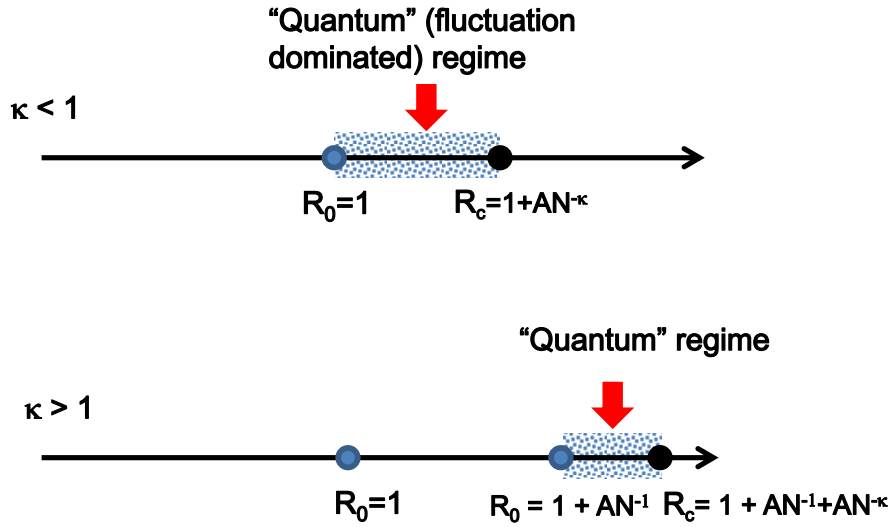


FIG. 3: The two possible scenarios for large N scaling. If $\kappa < 1$ (upper sketch) the $1/N$ self interaction shift is negligible with respect to the width of the quantum regime, thus the convergence to the deterministic limit is controlled by a single parameter $N^{-\kappa}$. The case $\kappa > 1$ (lower) is dominated by two scales: one that controls the distance of the transition point from its deterministic value, and the other that determines the width of the fluctuation dominated zone.

well-mixed (0d) and the mean field (∞ d) cases: in the first there is a pronounced quantum regime at finite N . In the second each point has infinite number of neighbors so the “effective N ” is infinite even if the number of individuals at each point is finite.

What remains is $d = d_u - 1$, namely three dimensions for SIS and five dimensions for SIR. In these cases, $\kappa = 2$, so the “quantum” regime has a very small width (of order N^{-2}) around the quantum transition point, which in turn is at a much larger distance (of order $1/N$) away from the deterministic transition point $R_0 = 1$. The situation is summarized in Fig. 3.

Although the transition point converges to $R_0 = 1$ in the infinite N limit, this convergence is slower than the rate in which the quantum zone shrinks around this point. This gives rise to two different scaling regimes, one of width $1/N$ and the second of width $1/N^2$. We can see this behavior, again, by studying M_N , the total mass of the infection, now as a function of R_0 , the “bare” reproductive number.

In the outer region, with width $\mathcal{O}(1/N)$, the mass obeys the scaling law

$$M_N = N^{\tau_M^{out}} \mathcal{G}_{out}(\tilde{\Delta}N). \quad (34)$$

Now, far from the transition point (say for fixed R_0 slightly below 1), at large enough N the dependence of M_N on this distance must approach its MF limit, $M_N \sim 1/(1 - R_0)$, independent of N . This implies that for large negative argument, $\mathcal{G}(x) \sim -1/x$, and that $\tau_M^{out} = 1$. Since the transition point is at $R_c \approx 1 + (A/N) + (B/N^2)$, where A and B are some constants, M_N must get large as $\tilde{\Delta}N$ approaches A . Since in this outer region, fluctuations are small, the incipient divergence of M is mean-field like, so \mathcal{G}_{out} diverges as $\mathcal{G}_{out} \sim c/(A - x)$, so that for R_0 near, but not too near R_c , M_N behaves as

$$M_N \approx \frac{C}{1 + A/N - R_0} \quad (35)$$

This behavior is demonstrated in Fig. 4, where N/M_N is plotted versus $\tilde{\Delta}N$, for SIS in three dimensions in the upper panel and for SIR in five dimensions in the lower. We see that there is a very slow convergence to an asymptotic curve. This slow convergence to the asymptotic scaling limit is reminiscent to what we encountered in the case of $d = d_u - 2$. The large N line is straight, but does not converge to zero at $R_0 = 1$, since the actual transition happens at $R_0 \approx 1 + A/N$. Although at large N , the distance of $R_0 = 1$ from the transition shrinks to zero one observes no “quantum” effects in the outer region since the width of the quantum regime shrinks even faster.

As we approach very close, of order a small fraction of $1/N^2$, to the phase transition point, the fluctuations become significant and M_N diverges as

$$M_N = AN^{-\tau_m} (R_c - R_0)^{-\gamma} \quad (36)$$

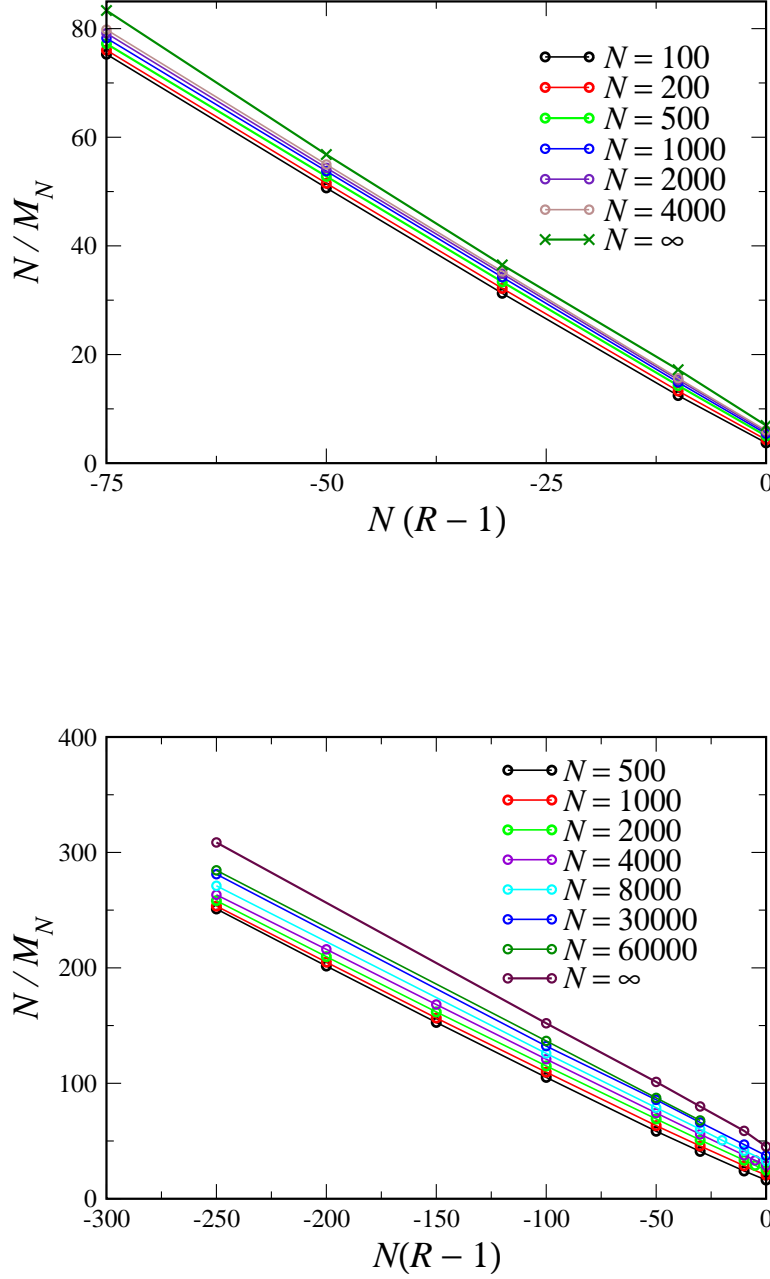


FIG. 4: Upper Panel: The inverse of the scaled “mass” of the aggregate, N/M_N , for the SIS model in $d = 3$ as a function of $N(R_0 - 1)$, for various N . The behavior for large $N(R_0 - 1)$ is consistent with $M_N = 1/(1 - R_0)$. The data labelled $N = \infty$ was obtained by fitting a quadratic curve in $N^{-1/3}$ to M_N for fixed $N(R_0 - 1)$ and extrapolating. This $N = \infty$ curve fits well to $M_N = N/(7.2 - N(R_0 - 1))$, corresponding to a shift in the critical R_0 by an amount $7.2/N$. Lower Panel: The inverse of scaled “mass” of the aggregate, N/M_N , for the SIR model in $D = 5$ as a function of $N(R_0 - 1)$, for various N . The behavior for large $N(R_0 - 1)$ is consistent with $M_N = 1/(1 - R_0)$. The data labelled $N = \infty$ was obtained by fitting a quadratic curve in $N^{-1/3}$ to M_N for fixed $N(R_0 - 1)$ and extrapolating. This $N = \infty$ curve fits well to $M_N = N/(47.6 - N(R_0 - 1))$, corresponding to a shift in the critical R_0 by an amount $47.6/N$.

where γ is the scaling exponent for the mass, which for DP in three dimensions is $\gamma \approx 1.24$ [20] and is approximately 1.2 for percolation in five dimensions. The general scaling law in the inner region, of width $\mathcal{O}(1/N^2)$ is then

$$M_N = N^{\tau_M^{in}} [\mathcal{G}_{in}(\Delta N^2)]^{-\gamma}. \quad (37)$$

where $\mathcal{G}_{in}(x)$ vanishes linearly at $x = 0$. For large negative argument, this has to match onto the outer behavior for $\tilde{\Delta}N \ll 1$. This is possible if $\mathcal{G}_{in}(x) \sim -Cx$ as $x \rightarrow \infty$ and $\tau_M^{in} = 2$.

Accordingly, the plot of $(N^{-2}M_N)^{-1/\gamma}$ vs. ΔN^2 shows the inner scaling function \mathcal{G}_{in} in the large N limit and goes linearly to zero at the transition point. This behavior is demonstrated in Fig. 5 for both the 3d SIS (upper panel) and the 5d SIR (lower panel) models.

FRONT VELOCITY

In the wake of Brunet and Derrida's [3] pathbreaking work on the large N behavior of the front velocity in Fisher-type systems, there has been an enormous amount of attention devoted to this issue, including a rigorous proof of the original heuristic arguments. It is thus natural to ask how this work relates to our current findings. The first thing to note is that the limits addressed here and the result of [3] are different. The Brunet-Derrida limit corresponds in our language to fixed Δ , $N \rightarrow \infty$, whereas we are interesting in the limit $\Delta \ll 1$, $N \gg 1$, $\Delta N^\kappa \sim \mathcal{O}(1)$.

We first investigate the behavior in the immediate vicinity of the transition point, restricting our attention to the 1d SIS model. In the immediate vicinity of the transition point, both the spatial correlation length, ξ_\perp , and the time correlation scale, ξ_\parallel diverge. It is expected then that the velocity will scale, in this regime, as the ratio of ξ_\perp to ξ_\parallel :

$$v \approx \frac{B_\perp N^{-\kappa(\nu_\perp - \frac{1}{2})} \Delta^{-\nu_\perp}}{B_\parallel N^{-\kappa(\nu_\parallel - 1)} \Delta^{-\nu_\parallel}} = B_v N^{\kappa(\nu_\parallel - \nu_\perp - \frac{1}{2})} \Delta^{\nu_\parallel - \nu_\perp} = B_v N^{-\kappa/2} (\Delta N^\kappa)^{\nu_\parallel - \nu_\perp} \quad (38)$$

Since $\nu_\parallel > \nu_\perp$, the velocity vanishes as the transition point is neared, just as in the classical theory. Furthermore, $\nu_\parallel - \nu_\perp - 1/2 > 0$, so the velocity increases with N for fixed Δ . This is consistent with the Brunet-Derrida asymptotic result, which also has the velocity rising with N at fixed Δ .

In the classical limit the front velocity is given by $v \sim \sqrt{\tilde{\Delta}}$, independent of N . One is tempted, then, to write, in analogy with our other scaling laws, $v \approx N^{-\kappa/2} \mathcal{H}(\tilde{\Delta} N^\kappa)$. The problem with this is that, while in the continuum classical limit, the velocity is proportional to $\sqrt{\tilde{\Delta}}$, on the lattice this is true only for small $\tilde{\Delta}$. To work with discrete agents and to define their local density one should implement some UV cutoff, so even for off-lattice models the relevant result is the one obtained for a lattice. The classical lattice velocity v_L satisfies the equation (see [22])

$$\frac{v_L}{\alpha\chi} \ln \left(\frac{v_L}{\alpha\chi} + \sqrt{1 + \left(\frac{v_L}{\alpha\chi} \right)^2} \right) + 1 - \sqrt{1 + \left(\frac{v_L}{\alpha\chi} \right)^2} = \frac{\beta\tilde{\Delta}}{\alpha\chi} \quad (39)$$

so that, for large $\tilde{\Delta}$, the velocity grows as $\tilde{\Delta}/\ln(\tilde{\Delta})$, as opposed to $\sqrt{\tilde{\Delta}}$. Thus, instead of trying to find a scaling relation for v , it is preferable to find a scaling relation for

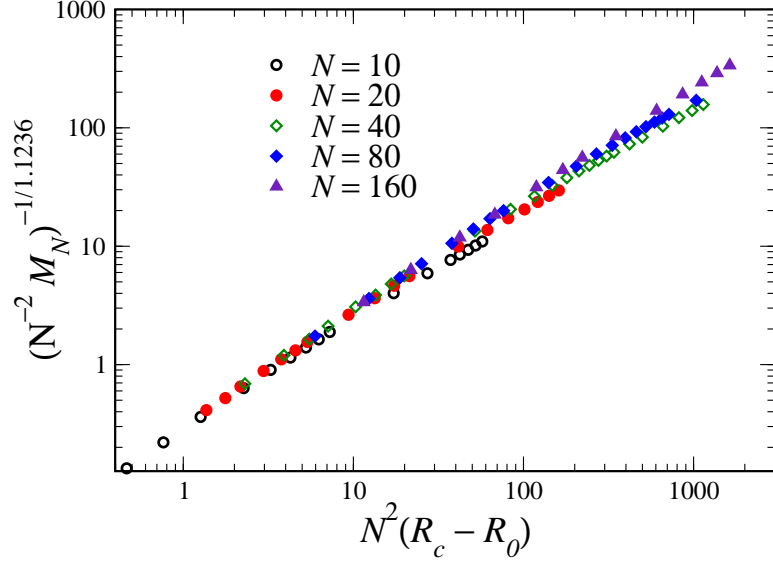
$$g(v) \equiv \sqrt{\frac{\alpha\chi}{\beta}} \left[\frac{v}{\alpha\chi} \ln \left(\frac{v}{\alpha\chi} + \sqrt{1 + \left(\frac{v}{\alpha\chi} \right)^2} \right) + 1 - \sqrt{1 + \left(\frac{v}{\alpha\chi} \right)^2} \right]^{1/2} \quad (40)$$

which, for $v = v_L$, is precisely equal to $\sqrt{\tilde{\Delta}}$. In Fig. 6, we show the scaling collapse of $g(v)N^{\kappa/2}$ versus $\tilde{\Delta}N^\kappa$. The Brunet-Derrida effect, namely the anomalously slow approach to the classical velocity, is apparent from this graph, where even for $\Delta N^{-\kappa} \sim 60$, the scaling curve is very far below the classical result.

In more detail, for large positive argument, the Brunet-Derrida result implies that

$$\mathcal{H}(x) \approx \sqrt{x} \left(1 - \frac{9\pi^2}{4 \ln^2 x} \right) \quad (41)$$

This corrected classical result is also show in Fig. 6, where we see quite good agreement, especially considering the relatively small values of N involved, compared to those necessary to achieve even semi-quantitative agreement with the Brunet-Derrida correction at $\tilde{\Delta} \sim \mathcal{O}(1)$.



//

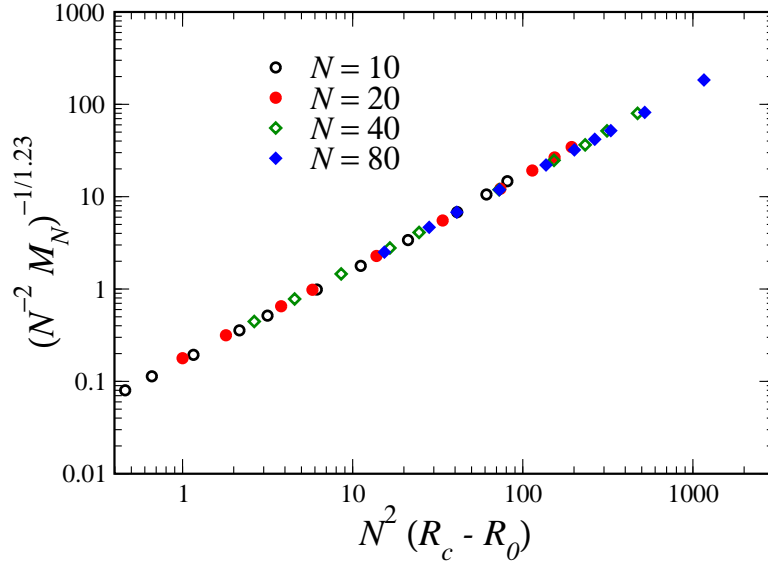


FIG. 5: (color online) Top: The scaled “mass” of the aggregate, $(M_N/N^2)^{-1/\gamma}$, as a function of the scaled “inner” variable $N^2(R_c - R_0)$, for the SIS model in $D = 3$. We used the value $\gamma = 1.236$. Bottom: The scaled “mass” of the aggregate, $(M_N/N^2)^{-1/\gamma}$, as a function of the scaled “inner” variable $N^2(R_c - R_0)$, for the SIR model in $D = 5$. We used the value $\gamma = 1.23$.

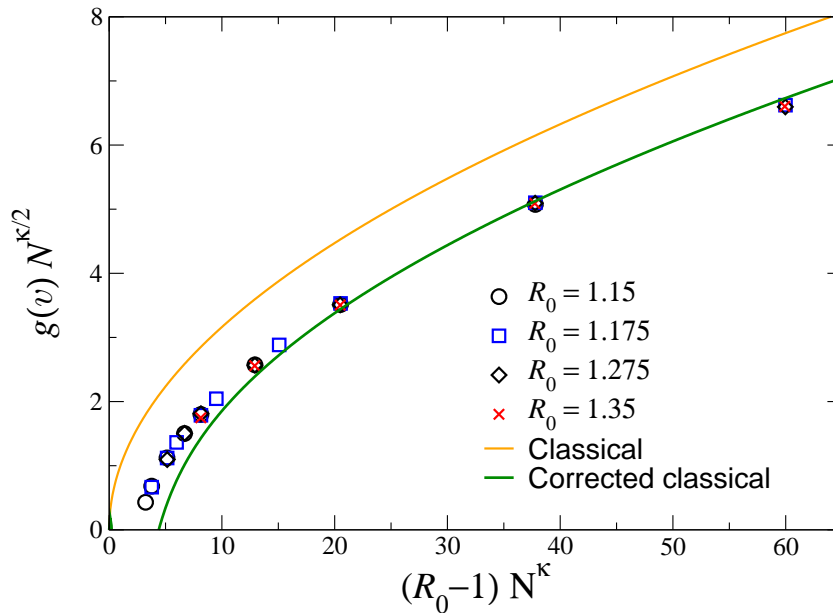


FIG. 6: The scaling collapse of the scaled transformed velocity, $g(v)N^{\kappa/2}$, where $g(v)$ is given in Eq. (40), versus $\tilde{\Delta}N^\kappa$ for the 1d SIS model, with $\beta = 1$, $\chi = 0.2$. The “classical” result is $\sqrt{(R_0 - 1)N^\kappa}$, whereas the “corrected classical” result is given by Eq. (41).

SUMMARY AND DISCUSSION

Along this paper we have studied, numerically and analytically, the convergence of the stochastic process to the deterministic rate equations when the number of particles is large. In spatially extended model there are two parameters that control the convergence: the number of particles per site N and the distance from the transition point. Together, these parameters yield a region of size $\Delta N^{-\kappa}$ above the phase transition point; within this region the system is dominated by demographic noise and the deterministic equations fail to describe it accurately.

The value of κ has been found before using an extensive analysis of zero dimensional [12, 19, 21, 23] and one dimensional [5] models. It turns out that this particular result may be derived directly, for any dimensionality, using the Ginzburg analysis. For the fundamental models considered here it depends only on the difference between d_u , the upper critical dimension, and d , via $\kappa = 2/(d_u - d)$.

Clearly, this general expression stems from the fact that the leading perturbative correction (i.e., the diagrams that lead to an infrared divergence in the highest dimension, which is thus the upper critical dimension) is proportional to $1/N$, since it involves an average over two noise terms, each is proportional to $1/\sqrt{N}$. This seems to be a generic property of stochastic processes and will be interesting to find out a model for which this general argument is not applicable.

Below $d_u - 2$ $\kappa < 1$, and the self-interaction shift is negligible at large N . In this case the point $R_0 = 1$ is peculiar: its normalized distance from the critical point (the distance divided by the width of the quantum regime) is N independent. Accordingly, the divergence of various observables at this point is determined solely by N^κ . This feature facilitates the numerics, since one can extract the value of the exponent without finding R_c . If $\kappa > 1$ this is no longer the case, and to locate the quantum regime one has to first identify the transition point.

Although the SIS and SIR processes serves us here as an archetypic stochastic processes that belong to the most pronounced equivalence classes of out-of-equilibrium transitions, they are also interesting models for epidemiologists. Several attempts have been made, recently, in order to understand better the role of fluctuations in individual-based, spatially structured epidemic models. The results presented here practically solve this problem for the case of subpopulations on a lattice considered in [24].

In the common case of zoonotic infections the pathogens first emerged from animal reservoirs, inducing a “stuttering

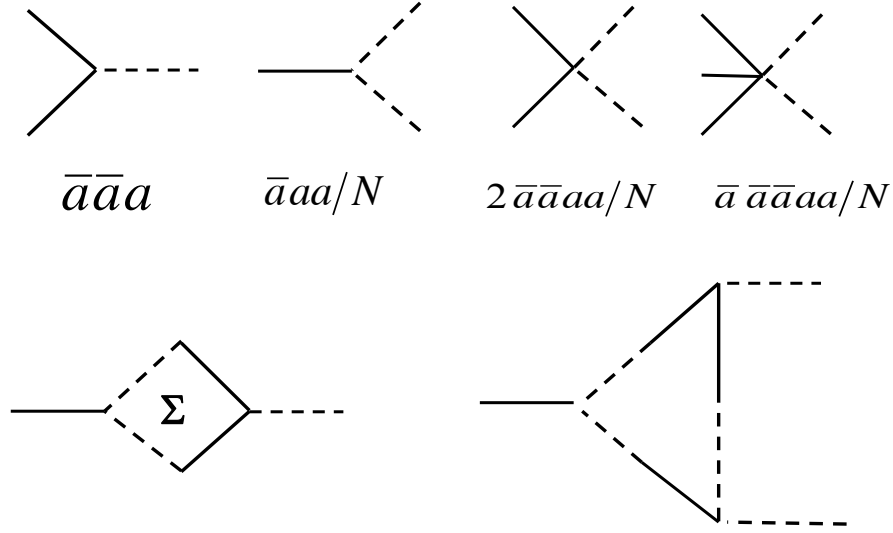


FIG. 7: Element of the diagrammatic perturbative expansion. The terms that appear in Eq. (20) (upper line), the self energy diagram Σ and the 1-loop correction to the three point vertex (lower part).

transmission” stage in which $R < R_c$, and reaching the phase of sustained transmission (human outbreak) only due to pathogen evolution (in human environment) to $R_0 > R_c$ [25]. If R_0 is growing slowly to larger value (as opposed to a major evolutionary step caused by a single mutation) the pathogen must cross the quantum region, where the size of the outbreak (the number of infections, and hence the chance for the next evolutionary step to occur) is simply $M_N(R)$. With an appropriate knowledge about the adaptation process of the pathogen, it will be quite easy to implement our results to obtain the chance of an outbreak.

ACKNOWLEDGEMENT

The authors thank Prof. Pierre Hohenberg for pointing out the work of Mon and Binder on the MF limit of equilibrium systems.

APPENDIX 1

Here we show some elements of the perturbative expansion of the action (19, 20) and the terms that determine the leading correction for large N , as explained in the text.

The elementary diagrams that appear in the perturbative expansion are shown in the upper part of Fig. 7. Of those, the first two appear in the Reggeon field theory and yield the one-loop renormalization of the mass and R_0 . The diagrams involved are presented in the lower part of Fig. 7.

With the bare propagator, Eq. (21), one can see that the leading correction to the mass behaves like

$$\frac{1}{N} \int \frac{q^{d-1} dq}{q^2 + m}.$$

This implies that q scales like \sqrt{m} and hence close to the transition the result is proportional to $\Delta^{-(2-d)/2}$, thus from this diagram one would get $\kappa = 2/(2-d)$ ($x = (2-d)/2$, $y = 1$, see text). The triangular diagram that provides the correction to the coupling constant scales like

$$\frac{1}{N^2} \int \frac{q^{d-1} dq}{(q^2 + m)^2},$$

so it corresponds to $\kappa = 4/(4-d)$. However, the corrections to the diffusion constant are given by the second derivative of the self-energy diagram with respect to the incoming momentum, and this contribution is proportional to

$$\frac{1}{N} \int \frac{q^{d-1} dq}{(q^2 + m)^2},$$

and this term yields the minimum value $\kappa = 2/(4 - d)$ given in Eq. (22).

* Electronic address: kessler@dave.ph.biu.ac.il

† Electronic address: shnerbn@mail.biu.ac.il

- [1] N. G. van Kampen, *Stochastic Processes in Physics and Chemistry* (North-Holland, Amsterdam, 1992).
- [2] See, e.g., D. A. Kessler and N. M. Shnerb, *J. Stat. Phys.* **127**, 861 (2007); O. Ovaskainen and B. Meerson, *Trends Ecol. Evol.* **25**, 643 (2010).
- [3] E. Brunet and B. Derrida, *Phys. Rev. E* **56**, 2597 (1997).
- [4] D. A. Kessler, Z. Ner and L. M. Sander, *Phys. Rev. E* **58**, 107 (1998).
- [5] D. A. Kessler and N. M. Shnerb, *J. Phys. A: Mathematical and Theoretical* **41**, 292003 (2008).
- [6] G. H. Weiss and M. Dishon, *Math. Biosci.* **11**, 261 (1971).
- [7] H. Hinrichsen, *Adv. Phys.* **49**, 815 (2000).
- [8] A. Pelissetto, P. Rossi and E. Vicari, *Phys. Rev. E* **58**, 7146 (1998).
- [9] K. K. Mon and K. Binder, *Phys. Rev. E* **48**, 2498 (1993).
- [10] W. O. Kermack and A. G. McKendrick, *Proc. Roy. Soc. A* **115**, 700 (1927).
- [11] R.M. Anderson and R.M. May, *Infectious Diseases in Humans*, Oxford University Press, Oxford (1992).
- [12] D. A. Kessler, *J. Appl. Prob.* **45**, 757 (2008).
- [13] R. Durrett and S.A. Levin, *Theor. Pop. Biol.* **46**, 361 (1994).
- [14] Y. Ben-Zion, Y. Cohen and N. M. Shnerb, *J. Theor. Biol.* **264**, 197 (2010).
- [15] R. A. Fisher, *Ann. Eugenics* **7**, 353 (1937); A. N. Kolmogorov, I. G. Petrovskii and N. S. Piskunov, *Selected Works of A. N. Kolmogorov*. V. M. Tikhomirov (Ed.), Kluwer Academic Publishers, 1991.
- [16] M. Doi, *J. Phys. A* **9**, 1465 (1976); L. Peliti, *J. Physique* **46**, 1469 (1985).
- [17] J.L. Cardy and U.C. Täuber, *J. Stat. Phys.* **90**, 1 (1998).
- [18] H-K Janssen and U.C. Täuber, *Annals of Physics* **315**, 147 (2005).
- [19] E. Ben-Naim and P. L. Krapivsky, *Phys. Rev.* **E69** 050901(R) (2004).
- [20] I. Jensen, *Phys. Rev. A* **45**, R563 (1992).
- [21] D.A. Kessler and N.M. Shnerb, *Phys. Rev.* **E. 76** 010901 (2007).
- [22] L. Pechenik and H. Levine, *Phys. Rev.* **E 59**, 3893 (1999).
- [23] A. Martin-Löf, *J. Appl. Probab.* **35**, 671 (1998).
- [24] W. M. Getz, et al., in Z. Feng, U. Dieckmann and S. Levin, eds., *Disease Evolution: Models, Concepts and Data Analyses*, DIMACS Series in Discrete Mathematics and Theoretical Computer Science 71, (American Mathematical Society, Providence, RI, 2006), p. 113.
- [25] R. Antia et. al., *Nature* **426** 658 (2003); J.O. Lloyd-Smith, et al., *Science* **326**, 1362 (2009).